Direct Observation of Complexation of Alkali Cations on Cyanide-Modified Pt(111) by Scanning Tunneling Microscopy

Youn-Geun Kim, Shueh-Lin Yau, and Kingo Itaya*

Contribution from the Itaya Electrochemiscopy Project, ERATO/JRDC, Research Institute of Electric and Magnetic Materials, Sendai 982, Japan, and Department of Applied Chemistry, Faculty of Engineering, Tohoku University, Sendai, Japan 982

Received July 7, 1995[⊗]

Abstract: In situ scanning tunneling microscopy was employed to examine the interfacial structure of a well-defined Pt(111) electrode in both acidic and alkaline solutions containing NaCN or KCN. A well-ordered $(2\sqrt{3}\times2\sqrt{3})$R30° CN-adlayer structure was observed at potentials in the double layer charging region. The adlayer consists of 6-membered-ring unit cells with cations coordinated in the center of the hexagon. The corrugation height of the center spot was found to be dependent on imaging conditions, becoming invisible under certain conditions, suggesting the absence of cyanide coordinated in the hexagonal ring. Bright spots were clearly observed in the center of the hexagonal ring when K^+ cations were introduced into the solution. These potential-dependent bright spots were attributed to strongly coordinated K^+ in the hexagonal ring of the adsorbed CN on Pt(111).

Introduction

In situ scanning tunneling microscopy (STM) has been employed extensively to study the structure of electrode surfaces such as single crystal Pt, Au, and Ag in electrolyte solution.[1] It is also well-demonstrated that in situ STM and in situ atomic force microscopy (AFM) have made it possible to determine the structures of various adlayers on these well-defined single crystal electrodes with atomic resolution. For example, the atomic adlayer structure of adsorbed anions such as I^-,[2−5] Br^-,[6] CN^-,[7] and sulfate/bisulfate[8−11] has been investigated. These novel techniques have produced significant impact to electrochemistry for the elucidation of the nature of electrode/electrolyte interfaces on the atomic level.[12] The adlayers described above are thought to be directly bonded to the electrode surface. According to the electrical double layer theory for the electrode/electrolyte interface,[13] the above mentioned work has indeed unfolded detailed structural information on the inner Helmholtz layer which is composed of specifically adsorbed species such as halides, sulfate/bisulfate, and water molecules. However, to our knowledge, no in situ STM investigation has previously been carried out for the elucidation of details of the outer Helmholtz layer. In general, chemical species such as solvated cations and anions in the outer Helmholtz layer might be expected to move rapidly to evade direct observation of such species by in situ STM as well as in situ AFM.

However, it is noteworthy that the adsorption of cations on top of the halide and CN^- adlayers formed on single crystal Pt electrodes has been extensively investigated by Hubbard and co-workers using an ex situ ultrahigh-vacuum electrochemical system.[14−16] Low-energy electron diffraction (LEED) and Auger spectroscopic data indicated that cations such as Li^+, Na^+, K^+, Cs^+, Ca^{2+}, Ba^{2+}, and La^{3+} are co-adsorbed on the well-defined CN adlayer on Pt(111).[15] It was also demonstrated that the cation exchange proceeds without loss or rearrangement of the CN adlayer.[15] Detailed structure analysis of the CN adlayer on Pt electrodes was also investigated by ex situ LEED[14−16] as well as in situ infrared spectroscopy (IR),[17−20] sum frequency generation,[21] and STM.[9] It is believed that the adsorbed CN linearly binds to the Pt substrate predominantly through its C-end. These results encouraged us to explore the use of in situ STM to probe the nature of the electrical double layer at the electrode/electrolyte interface.

Real space structures of the CN adlayer on Pt(111) were determined by ex situ LEED,[14,15] which showed that two different adlattices consisting of the CN^- anion and its protonated form (CNH) exist with the structures of $(2\sqrt{3}\times2\sqrt{3})$-R30° (hereafter referred to as $2\sqrt{3}$) and $(\sqrt{13}\times\sqrt{13})$R14°, depending on the electrode potential and pH. The latter structure

* Address correspondence to this author at Tohoku University.

[⊗] Abstract published in *Advance ACS Abstracts,* December 1, 1995.

(1) For a recent review, see: Siegenthaler, H. In *Scanning Tunneling Microscopy II*; Wiesendanger, R., Guntherodt, H.-J., Eds.; Springer-Verlag: New York, 1992; pp 7−49.
(2) Yau, S.-L.; Vitus, C. M.; Schardt, B. C. *J. Am. Chem. Soc.* **1990**, *112*, 3677.
(3) Gao, X.; Weaver, M. J. *J. Am. Chem. Soc.* **1992**, *114*, 8544.
(4) Sugita, S.; Abe, T.; Itaya, K. *J. Phys. Chem.* **1993**, *97*, 8780.
(5) Yamada, T.; Batina, N.; Itaya, K. *J. Phys. Chem.* **1995**, *99*, 8817.
(6) Tanaka, S.; Yau, S.-L.; Itaya, K. *J. Electroanal. Chem.* **1995**, in press.
(7) Stuhlmann, C.; Villegas, I.; Weaver, M. J. *Chem. Phys. Lett.* **1994**, *219*, 319.
(8) Magnussen, O. M.; Hagebock, J.; Hotlos, J.; Behm, R. J. *Faraday Discuss. Chem. Soc.* **1992**, *94*, 329.
(9) Edens, G. J.; Gao, X.; Weaver, M. J. *J. Electroanal. Chem.* **1994**, *375*, 357.
(10) Funtikov, A. M.; Linke, U.; Stimming, U.; Vogel, R. *Surf. Sic.* **1995**, *324*, L343.
(11) Wan, L.-J.; Yau, S.-L.; Itaya, K. *J. Phys. Chem.* **1995**, *99*, 9507.
(12) Bard, A. J.; Abruna, H. D.; Chidsey, C. E.; Faulkner, L. R.; Feldberg, S. W.; Itaya, K.; Majda, M.; Melroy, O.; Murray, R. W.; Porter, M. D.; Soriaga, M. P.; White, H. S. *J. Phys. Chem.* **1993**, *97*, 7147.
(13) Parsons, R. In *Modern Aspects of Electrochemistry*; Bockris, J. O. M., Conway, B. M., Eds.; Butterworths Scientific Publications: London, 1954; Vol. 1, pp 103−131.
(14) Stickney, J. L.; Rosasco, S. D.; Salaita, G. N.; Hubbard, A. T. *Langmuir* **1985**, *1*, 66.
(15) Rosasco, S. D.; Stickney, J. L.; Salaita, G. N.; Frank, D. G.; Katekaru, J. Y.; Schardt, B. C.; Soriaga, M. P.; Stern, D. A.; Hubbard, A. T. *J. Electroanal. Chem.* **1985**, *188*, 95.
(16) Frank, D. G.; Katekaru, J. Y.; Rosasco, S. D.; Salaita, G. N.; Schardt, B. C.; Soriaga, M. P.; Stern, D. A.; Stickney, J. L.; Hubbard, A. T. *Langmuir* **1985**, *1*, 587.
(17) Kitamura, F.; Takahashi, M.; Ito, M. *Chem. Phys. Lett.* **1986**, *130*, 181.
(18) Kawashima, H.; Ikezawa, Y.; Takamura, T. *J. Electroanal. Chem.* **1991**, *317*, 257.
(19) Paulissen, V. B.; Korzeniewski, C. *J. Phys. Chem.* **1992**, *96*, 4563.
(20) Kim, C. S.; Korzeniewski, C. *J. Phys. Chem.* **1993**, *97*, 9784.
(21) Guyot-Sionnest, P.; Tadjeddine, A. *Chem. Phys. Lett.* **1990**, *172*, 341.

0002-7863/96/1518-0393$12.00/0

was found to appear at negative potentials.[16] In situ STM was more recently employed to examine the CN adlayer on Pt(111).[7] It was reported that six CN functional groups form a hexagonal ring with an additional CN in the center of the ring (see Figure 8a). This structure differs from that suggested on the basis of the ex situ LEED data, although both structures had the same $(2\sqrt{3}\times 2\sqrt{3})$R30° symmetry. Although the arrangement of the adsorbed CN was revealed by in situ STM, the adsorption of cations on the CN adlayer described above was not discussed in the previous paper.[7]

In situ STM observations of complexation of alkali cations such as Na^+ and K^+ with the CN adlayer on Pt(111) is, for the first time, described in this paper. It is clearly shown that these cations are trapped at the center of the hexagonal CN rings. A new structure is proposed for the CN adlayer on Pt(111). Effects of protonation on the adlayer structure are described. Potential-dependent dynamics of K^+ complexation is also described.

Experimental Section

A Pt single crystal bead (3 mm in diameter) was made at one end of a pure Pt wire (1 mm in diameter). The well-prepared Pt bead consisted of (111) facets in an octahedral configuration. These (111) facets usually gave well-defined terrace and step structures.[6,22] The atomically flat terraces which usually appeared with a width greater than 50 nm were important for achieving STM atomic resolution. The orientation of the single crystal was determined with a laser diffraction technique. For voltammetric measurements, the Pt(111) single crystal was mechanically exposed by polishing with successively finer grade Al_2O_3 powder ranging from 2 to 0.05 μm. The Pt(111) electrode was finally annealed by a H_2/O_2 flame for at least 3 h to remove surface damages caused by mechanical polishing. STM imaging indicated that the mechanically polished Pt(111) electrode still showed well-defined steps and terraces, although the width of the terraces decreased to an average dimension of 10 nm. A flame-annealing and quenching procedure was used to expose the well-defined (111) surface into solution. The quenching was done in hydrogen-saturated Millipore water after allowing the glowing electrode to cool by briefly holding the electrode in the H_2 stream (ca. 2−3 s) prior to dipping it into the water. The cyclic voltammogram (CV) for the Pt(111) electrode in 0.1 M $HClO_4$ showed consistently the characteristic butterfly feature,[23,24] indicating that the well-ordered Pt(111) was successfully prepared by the procedure described above. The clean Pt electrode protected by a droplet of water was quickly transferred into a 0.1 mM NaCN solution to form the CN adlayer and then into an electrochemical cell for voltammetric and STM studies.

Ultrapure NaCN and $NaClO_4$ were obtained from Cica Merck Chemicals, and Millipore water was used to prepare all solutions. NaOH and KOH solutions were used to adjust the pH to 9.5. The concentration ratio of CN^- to neutral HCN is expected to be roughly 1/2 at this pH. The cyclic voltammetry was performed in an electrochemical cell with three compartments, utilizing a reversible hydrogen reference electrode (RHE) in either 0.1 M $HClO_4$ or 0.1 M $NaClO_4$ (pH 9.5) containing no cyanide. A saturated calomel electrode (SCE) was used to calibrate the RHE in the solutions of different pH values. A Pt wire was used as the counter electrode.

The potential was controlled by a Hokuto potentiostat (Tokyo). A NanoScope III STM (Digital Instruments, Santa Barbara, CA) was used with a modified electrochemical cell employing an RHE reference and a Pt counter electrode. The tip was a W wire (0.03 in.) electrochemically etched in a 1 M KOH bath. The W tips were partially coated with transparent nail polish to minimize the faradaic current.

Results and Discussion

Voltammetry in Alkaline and Acidic Cyanide Solutions. Although much work has previously been performed studing cyanide adlayers on Pt electrodes, the features contained in cyclic voltammograms for single crystal electrodes exposed to solutions containing cyanide are not well-understood.[14−21] Therefore, we initially investigated voltammetric behavior of well-defined Pt(111) in 0.1 M $NaClO_4$ (pH 9.5) and 0.1 M $HClO_4$, both in the absence of CN^-. These data are shown in Figures 1a and 2a, respectively. The electrode potential is shown with respect to the reference electrodes of both the RHE (lower scale) and SCE (upper scale). These CV curves represent pseudo-steady-state voltammograms obtained after 2−3 cycles. In the alkaline solution (Figure 1a), the highly reversible wave at 0.85 V vs RHE is present and attributed to the specific adsorption of anions on Pt(111).[24,25] The irreversible oxidation peak at 1.1 V obtained during a more anodic scan to 1.3 V is interpreted as being due to the adsorption of hydroxide (−OH) on Pt(111). The reversible hydrogen adsorption and desorption reactions can be seen in the potential range between 0.15 and 0.5 V. All the voltammetric peaks observed in perchloric acid (Figure 2a) are identical with those obtained by other groups for well-ordered Pt(111) and serve as the well-known finger print.[23,24] These results clearly indicate that the Pt(111) surface used in the present study can be characterized as an ideal one. After recording the CV's shown in Figures 1a and 2a, the Pt-(111) electrode with a droplet of pure electrolyte solution was transferred into a second electrochemical cell containing cyanide ions.

It is clearly seen in Figure 1b that the presence of CN^- (solid line) eliminates the reversible peak at 0.85 V as well as the irreversible oxidation peak at 1.1 V observed in the absence of

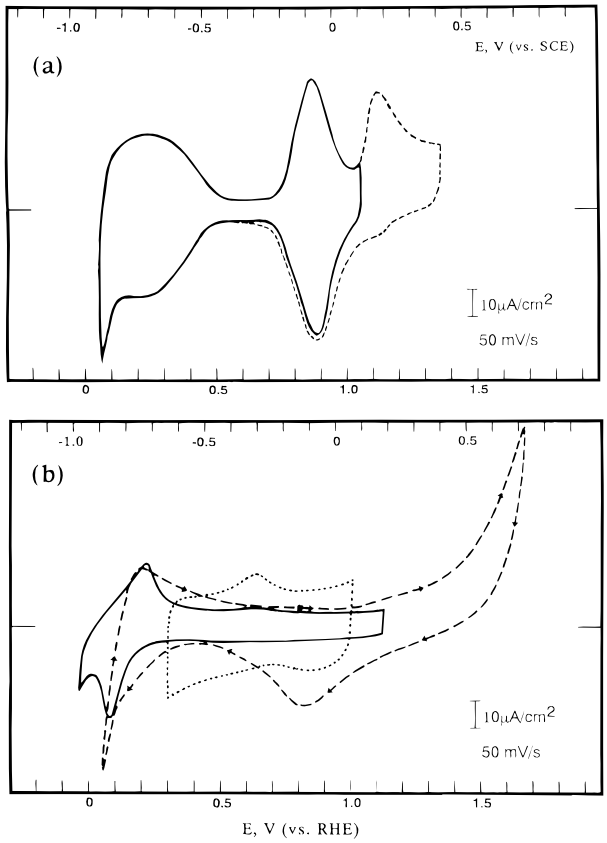

Figure 1. Cyclic voltammograms for Pt(111) in 0.1 M $NaClO_4$ (pH 9.5) (**a**) and 0.1 mM NaCN + 0.1 M $NaClO_4$ (pH 9.5). (**b**) The broken curves were obtained under more positive potential excursions. The dotted line in (**b**) represents an enlarged (×4) charging curve in the double layer region. The scan rate was 50 mV/s.

(22) Itaya, K.; Sugawara, S.; Sashikata, K.; Furuya, N. *J. Vac. Sci. Technol.* **1990**, *A8*, 515.
(23) Clavilier, J.; Rodes, A.; El Achi, K.; Zamakhchari, M. A. *J. Chim. Phys.* **1991**, *88*, 1291.
(24) Wagner, F. T.; Ross, P. N. *J. Electroanal. Chem.* **1988**, *250*, 301.
(25) Morallón, E.; Vázquez, J. L.; Aldaz, A. *J. Electroanal. Chem.* **1992**, *334*, 323.

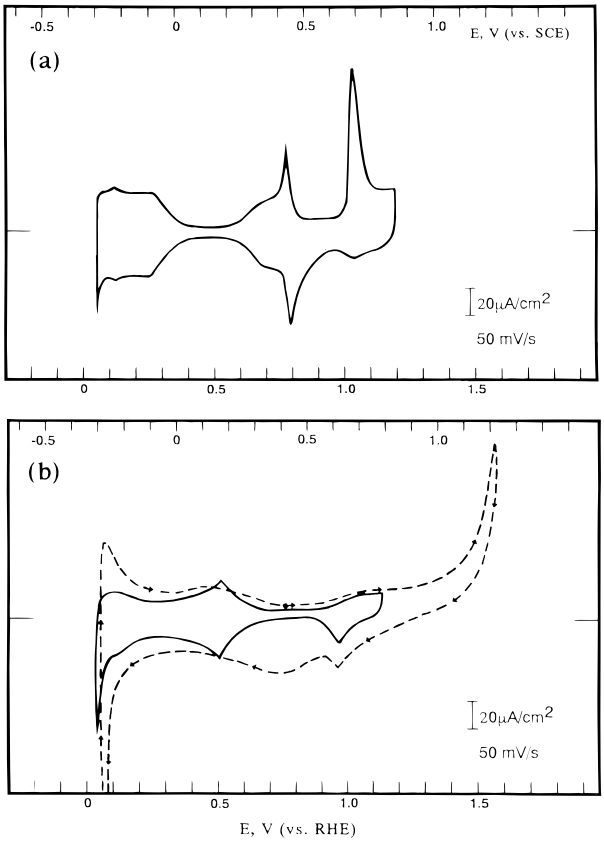

Figure 2. Cyclic voltammograms for Pt(111) in 0.1 M $HClO_4$ (**a**) and 0.1 mM NaCN + 0.1 M $HClO_4$ (**b**). The broken curve was obtained when the anodic limit was gradually made more positive. The scan rate was 50 mV/s.

CN^- (Figure 1a). The presence of CN^- gives rise to a featureless double layer charging region extending from 0.3 to 1 V. It is also noticed that the hydrogen adsorption and desorption peaks are almost completely suppressed in the presence of CN^-. Note that a reduction peak appears at 0.1 V near the onset of the hydrogen evolution reaction. This might be due to a partial desorption of the adsorbed CN^- and to the simultaneous adsorption of hydrogen on Pt(111), although such a pronounced peak was not found on polycrystalline Pt electrodes.[19] After subtracting the double layer charging current, a charge density of 65 ± 5 $\mu C/cm^2$ was obtained for the reduction peak at 0.1 V. This is roughly equal to 40% of the theoretical charge (ca. 160 $\mu C/cm^2$) for hydrogen adsorption in the potential region between 0.1 and 0.5 V on the clean Pt-(111) surface.[26] Note that, using ex situ LEED[16] and in situ STM,[9] the $2\sqrt{3}$ structure of the CN adlayer was found to be converted to the $(\sqrt{13}\times\sqrt{13})R14°$ or (2×2) structure in negative potentials. The result shown in Figure 1b suggests that the peak observed at 0.1 V might involve a structural transition of the CN adlayer. The CV shown in the dotted line in Figure 1b was recorded with a fourfold increase in current scale. The broad anodic peak at 0.62 V appears to be irreversible at the scan rate of 50 mV/s. The same peak with an identical shape and height was also found in a 0.1 mM KCN + 0.1 M $KClO_4$ (pH 9.5) solution. It is shown below that this peak is associated with the complexation of alkali cations such as Na^+ and K^+ with the CN adlayer, rather than the structural transition of the CN adlayer as described previously.[16]

A further anodic potential excursion to 1.6 V led to the oxidation of CN to OCN^- or CO_2 (broken line) as indicated in an in situ IR study.[17] It is also clear that the oxidation of Pt occurred during the anodic excursion, resulting in the disappearance of the quasireversible peak at 0.1 V due to the disordering of the Pt(111) surface.[22]

(26) Feliu, J. M.; Orts, J. M.; Gomez, R.; Aldaz, A.; Clavilier, J. *J. Electroanal. Chem.* **1994**, *372*, 265.

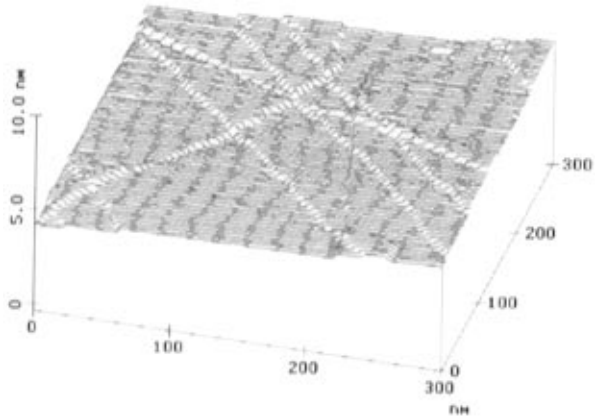

Figure 3. STM line scans of a Pt(111) facet acquired in 0.1 mM NaCN + 0.1 M $NaClO_4$ (pH 9.5). The electrode potentials of Pt(111) and the tip were 0.7 and 0.6 V vs RHE, respectively. The tunneling current was 5 nA.

In the acidic solution, the presence of CN^- completely changes the CV features as shown in Figure 2b. The butterfly peaks and the irreversible oxidation peak at 1.1 V have disappeared, similarly to the case in alkaline solution. On the contrary, the peaks due to the hydrogen adsorption and desorption reactions still can be seen in the cathodic region, suggesting that hydrogen adsorption sites are not entirely blocked by the adsorption of CN^- in the acidic solution. It is also expected that a partial desorption of the adsorbed CN^- might take place in this potential range. A charge density of ca. 70 $\mu C/cm^2$ was found in a potential range between 0.05 and 0.7 V. An anodic scan from 0.75 to 1.5 V results in a precipitous increase in the anodic current (broken line). The subsequent cathodic scan gives rise to reduction peaks at 0.95 and 0.75 V, which can be associated with the reduction of oxide species on the Pt electrode. The reversible feature at 0.5 V for a well-ordered Pt(111) electrode is no longer present in the CV due to surface roughening.

Topographic STM Imaging of the Pt(111) Facet. The typical surface structure of a Pt(111) facet obtained at 0.75 V in a 0.1 mM NaCN + 0.1 M $NaClO_4$ (pH 9.5) solution is shown in Figure 3. The surface is characterized by a widely extended terrace and step structure. Each line corresponds to a monatomic step with a height of 0.23 nm. The orientations of the steps mostly seem to parallel the close-packed directions of the (111) substrate. It was not difficult to find an area where the width of an atomically flat region was more than 100 nm. These surface features are consistent with our previous reported results.[6,22] It was found in this study that high-resolution STM images discerned the atomic structure of the CN adlayer over terraces, indicating that Pt(111) terraces were uniformly covered by chemisorbed CN species. The uniform appearance of the terraces also suggests that the CN adlayer effectively inhibited the adsorption of organic contaminants which might occur during the transfer of Pt sample through the ambient. The chemisorbed CN species were also stable toward oxidation in the ambient. The Pt electrode emmersed from the solution containing CN^- was strongly hydrophilic, which is likely to be due to the hydration of the coadsorbed cations. This hydrophilicity was also pointed out in the previous work.[16]

Atomic STM Imaging in Alkaline NaCN and KCN Solutions. An atomically resolved STM image acquired in an

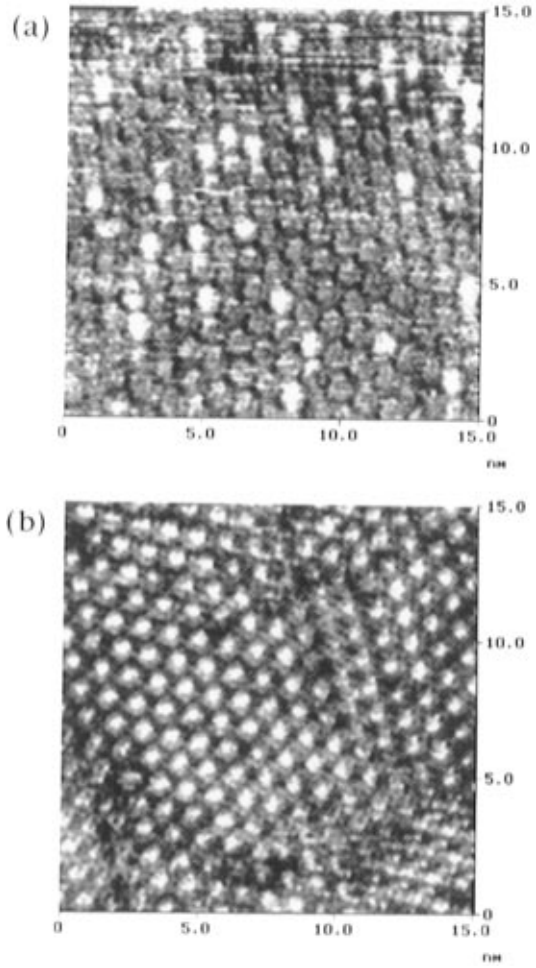

Figure 4. High-resolution STM images of the $(2\sqrt{3}\times2\sqrt{3})$R30° structure found on Pt(111) in the solutions containing 0.1 mM NaCN (**a**) and 0.1 mM KCN (**b**) at 0.7 V. These images were acquired with −100 mV bias voltage and 5 nA tunneling current.

alkaline CN solution containing Na^+ cations is shown in Figure 4a. The image was obtained in the constant current mode using a tunneling current of 13 nA. The electrode potentials of Pt(111) and the tip were 0.7 and 0.6 V, respectively. Under these experimental conditions well-arranged hexagonal rings, aligned in a direction 30° rotated from the close-packed directions of the Pt(111) lattice, are observed. The 0.95 ± 0.02 nm distance between the nearest neighbor hexagonal rings, as measured from their centers, is roughly twice as large as the $\sqrt{3}$ lattice spacing of the Pt (0.2778 nm). This ordered atomic feature can be characterized as the $(2\sqrt{3}\times2\sqrt{3})$R30° structure, which has the same symmetry as that proposed by the LEED[14−16] and in situ STM studies.[7]

Note that Weaver and co-workers reported an STM image (see Figures 3 and 4 in ref 7) which was interpreted as the $(2\sqrt{3}\times2\sqrt{3})$R30°−7CN structure with cyanides bound in symmetric atop sites surrounded by hexagonal rings of near-top CN.[7] However, we found that some sparsely distributed bright spots are located nearly in the centers of the hexagonal rings of CN. As more detailed atomic images will be discussed below, the bright spots in Figure 4a are tentatively attributed to coadsorbed Na^+ cations on the CN adlayer with $2\sqrt{3}$ symmetry.

In order to elucidate the role of cations, we carried out STM experiments in solutions containing K^+ cations. The image shown in Figure 4b was obtained in a 0.1 mM KCN + 0.1 M $KClO_4$ (pH 9.5) solution. The imaging conditions were identical to those for Figure 4a. It was surprising to find that the bright spots appear almost uniformly over the entire imaged area. At

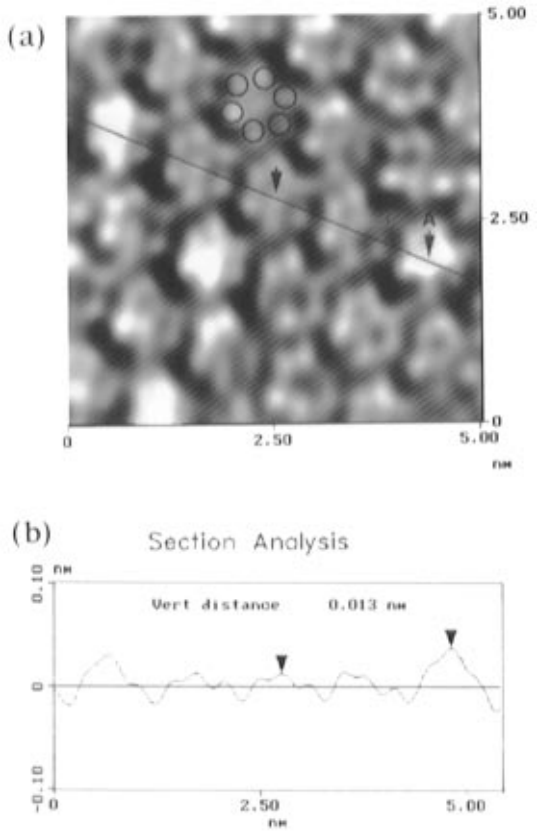

Figure 5. High-resolution STM images of the ordered $(2\sqrt{3}\times2\sqrt{3})$-R30° structure observed in the solution containing 0.1 mM NaCN (**a**) and the cross section profile (**b**). The image was obtained at 0.7 V, and the tip potential was 0.6 V. The imaging conditions were the same as for Figure 4. A Fourier transform filtering was applied.

a superficial glance, the image seems to be composed of only the bright spots without clear appearance of the hexagonal ring. This is due to the relatively large corrugation height of ca. 0.035 nm observed on the bright spot. The interatomic distance between two nearest bright spots is equal to the $2\sqrt{3}$ spacing. It can be concluded that the bright protrusions form the well-ordered $2\sqrt{3}$ array. The bright spots are likely attributable to the coadsorbed K^+ on the CN adlayer. The ex situ UHV studies indicated that K^+ was more strongly adsorbed on the CN adlayer than Na^+.[15]

More information regarding the structure of the adsorbed CN^- and cations in solutions containing Na^+ or K^+ was revealed in higher resolution STM images. Figure 5a shows a high-resolution image acquired in 0.1 mM NaCN. As seen previously, a few sparsely distributed CN hexagons exhibit bright center spots. It is also observed that the other remaining hexagonal ring centers without a bright spot have intensities similar to that of the surrounding six spots. The corrugation profile shown in Figure 5b is the cross section along the line shown in Figure 5a which depicts these observations. A difference of 0.013 nm exists between two different center spots in each hexagonal ring. Profile analysis indicates that the darker center spot shows roughly the same corrugation amplitude as the surrounding spots. These results except the existence of the brighter spot are consistent with the previous STM results.[7] In contrast, the central protrusion of A appears noticeably higher than the neighboring ones. Evidently, neither different registries of CN nor imaging artifacts can explain the rather distinct brighter spots.

On the other hand, the image acquired in 0.1 mM KCN shown in Figure 6a uniformly showed spots even brighter than the

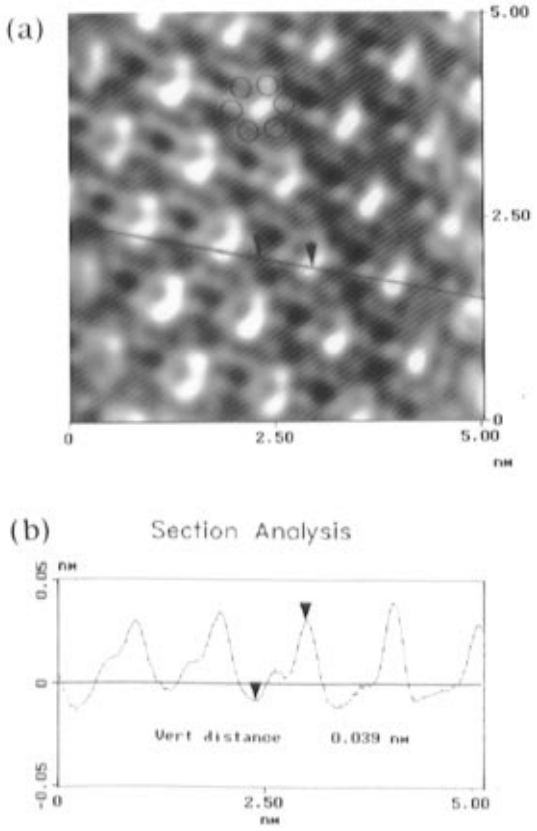

Figure 6. High-resolution STM images of the ordered ($2\sqrt{3}\times2\sqrt{3}$)-R30° structure observed in the solution containing 0.1 mM KCN (**a**) and the cross section profile (**b**). The image was obtained at 0.7 V, and the tip potential was 0.6 V. The imaging conditions were the same as for Figure 4. A Fourier transform filtering method was applied.

surrounding six spots under imaging conditions identical to those for Figure 5. It can be seen that the corrugation amplitude of the center spots is roughly three times larger than that observed in the NaCN solution, indicating that the corrugation height of the center spots depends on the cation type. Despite the fact that these central protrusions always appear higher than the neighboring atoms, it is worth noting that their corrugation amplitudes depended on the STM imaging conditions, including the magnitudes of tunneling current and bias voltage. It was found that a decrease in the tip-to-sample separation brought about by lowering the bias voltage or by increasing the tunneling current usually resulted in hollow hexagonal patterns in STM images obtained in the NaCN solution. Figure 7 shows an unfiltered STM image of this hollow hexagonal pattern. This image (5 × 5 nm) was acquired in 0.1 mM NaCN + 0.1 M $NaClO_4$ (pH 9.5) at 0.6 V with a bias voltage of −50 mV and a tunneling current of 20 nA. It is clear that the center spots are now essentially invisible in the image shown in Figure 7. It is also important to note that the brighter center spot attributed to Na^+ as described above also disappears. The STM image reversibly revealed the brighter central spots if the imaging conditions were switched back to those used in Figure 5a. The disappearance of the central protrusions could result from tip−sample interactions, which push the coadsorbed cation species out of the imaged area. However, given the high reversibility of the STM imaging, it is more likely that this phenomenon is attributed to the selective imaging of the adsorbates by the STM. A similar transparency was demonstrated for the iodine[3] and sulfate/bisultate[8] adlayers. Nevertheless, the result shown in Figure 7 strongly suggests that there is no cyanide in the center of the hexagonal ring. Even the darker center spot appearing in Figure 5a cannot be attributed to CN.

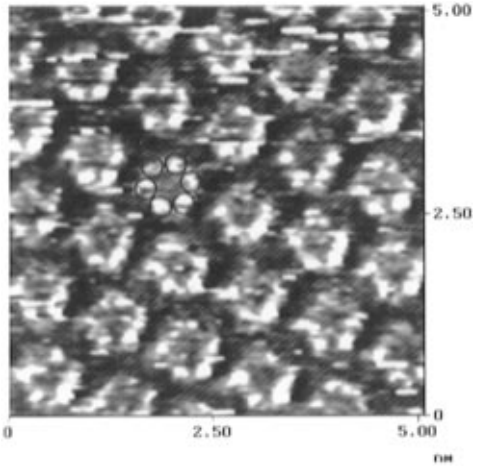

Figure 7. Unfiltered high-resolution STM image (5 × 5 nm) of the hollow CN hexagonal arrangement. The image was obtained in 0.1 mM NaCN and 0.1 M $NaClO_4$ (pH 9.5). The electrode potentials of Pt(111) and the tip were 0.6 and 0.5 V, respectively. The tunneling current was 20 nA.

Based on the results described above, three model structures are presented in Figure 8 to outline atomic arrangements of the adsorbed CN and K^+ on Pt(111). The model structure shown in Figure 8a is essentially a replica of the model proposed by Weaver and co-workers,[7] in which the center spot was attributed to the adsorbed CN. However, the image shown in Figure 7 suggests that the adsorbed CN is not located in the center of the six-membered ring as described above. Figure 8b is a new model where the adsorbed CN in the center is removed.

It is interesting to note that the six-membered ring is similar in structure to crown ethers. Crown ethers are known to effectively complex with the alkali metal cations.[27] The configuration of the CN adlayer is such that the C is bound to the Pt electrode with the N facing the solution side. Each nitrogen atom contains a lone pair of electrons which is expected to act as a binding site similar to the oxygen atoms in crown ethers. Furthermore, the binding constant of the crown ether and alkali metal is dominated by their size compatibility.[27] For example, the crown-6 ether selectively binds with K^+ while the crown-5 and crown-4 favor binding with Na^+ and Li^+, respectively.[27] We believe that K^+ cations are more strongly bounded in the center of the CN ring than Na^+ because of a similar size effect.

The model shown in Figure 8b cannot directly explain the appearance of the hexagonal ring with the additional center spot having a corrugation height similar to that of the six-membered ring as shown in Figures 4a and 5. However, we suppose that proton (H^+) or hydronium cations (H_3O^+) should be coordinated in the center of the ring. Such hydronium cations are expected to appear as the center spot, but they became transparent in the STM imaging under certain conditions as described in Figure 7. According to the model shown in Figures 8b and 8c, the surface coverages of CN and of K^+ are 6/12 and 1/12, respectively. (There are 12 Pt atoms in the unit cell.) It is noteworthy that the latter value is one-half of that predicted by the model proposed by Hubbard and co-workers.[14−16] They proposed a model structure with a K^+ surface coverage of 2/12, where two K^+ ions occupied the unit cell, and experimentally confirmed this value by Auger spectroscopy. If those UHV results are taken for granted, it would seem possible that the in situ STM imaging might not be able to see the additional K^+ in the unit cell which is expected to be weakly bonded to the

(27) Frensdorff, H. K. *J. Am. Chem. Soc.* **1971**, *93*, 600 and references therein.

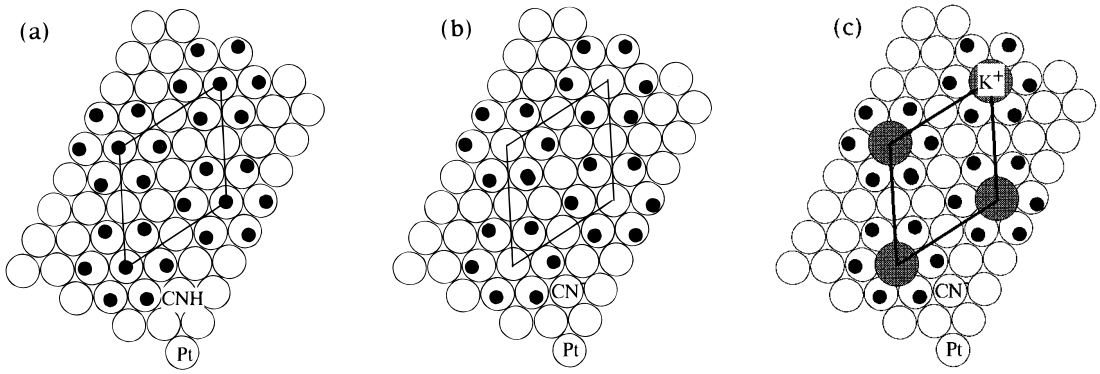

Figure 8. Three ball models of the $(2\sqrt{3}\times2\sqrt{3})$R30° structure.

CN adlayer by a simple electrostatic interaction to maintain charge neutrality. Further work is needed to clarify this discrepancy.

Atomic STM Imaging in 0.1 M $HClO_4$. We have further investigated the CN-adlayer structure in a $HClO_4$ solution in the absence of an excess amount of alkali cations in order to obtain a better understanding of the center spot. Figure 9 shows two typical STM images acquired in the solution of 0.1 mM NaCN + 0.1 M $HClO_4$ at 0.8 V (see Figure 2b). A highly ordered atomic array is clearly revealed. The lower region located at the right-hand side of the STM image in Figure 9a is attributed to monatomic steps with a step height of 0.23 nm. A close-up view of the terrace obtained by applying a 2D filtering method shown in Figure 9b reveals a clear atomic structure. The unit cell outlined in Figure 9b is identified as the $(2\sqrt{3}\times2\sqrt{3})$R30° structure. The CN arrangement resembles the reported STM results,[7] in that groups of seven CN adsorbates form centered hexagonal patterns. The central protrusions show a similar corrugation height with respect to those of the neighboring ones under the tunneling condition described above. However, the appearance of the center spot was also found to be dependent on the tunneling conditions. The center spot became unclear when the tunneling current was increased. This observation again suggests that the center spot is not due to the cyanides. Hydronium cations are likely located in the center of the hexagonal ring to compensate for the negative charge of the CN adlayer.

When the electrode potential was scanned negatively from 0.8 to 0.3 V, it was interestingly found that the in situ STM revealed a new CN-adlayer structure with a long-range order. A close-up view is shown in Figure 10a, accompanying a ball model (Figure 10b) which is identified as a $(\sqrt{7}\times\sqrt{7})$R19° structure. The unit cell contains four CN adsorbates and results in a 0.57 coverage, which is slightly lower than that of the $2\sqrt{3}$ structure ($\theta = 0.583$) found at more positive potentials as described above. The model indicates that the corner CN's occupy the on-top sites, whereas the remaining CN's rest on the near-top sites or possibly 2-fold bridge sites. The model is in good agreement with the corrugation of the STM image shown in Figure 10. It can be seen that the STM image shows the brightest corner spots, the weaker near-top ones, and the weakest spots within the unit cell. The weakest spot seems to correspond to the cyanide on the 2-fold bridge site. The unfavorable asymmetric binding geometries of the CN might be due to repulsive interactions among the CN. The new structure was found in a potential range between 0.2 and 0.4 V. A small amount of CN desorption and a structural transition of the CN adlayer are expected to occur at 0.5 V in CV shown in Figure 2b. The adsorption of H is also believed to occur in the same potential range. However, the structure shown in Figure 10 was consistently observed in the above potential range,

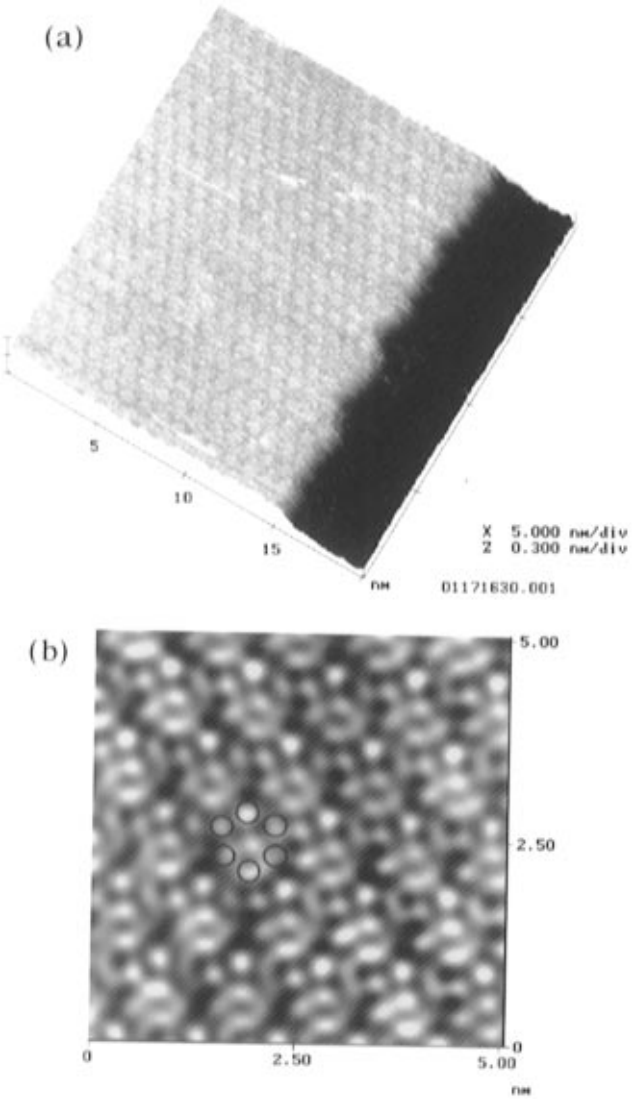

Figure 9. Large-scale (**a**) and high-resolution (**b**) STM images of the $(2\sqrt{3}\times2\sqrt{3})R30°$ structure on Pt(111) in 0.1 mM NaCN + 0.1 M $HClO_4$. The Pt and tip potentials were held at 0.8 and 0.7 V, respectively, and the tunneling current was 10 nA.

suggesting that the structural transition occurred in a rather narrow potential range near 0.5 V. The additional hydrogen adsorption did not seem to cause further restructuring of the CN adlayer. The uncoordinated Pt sites shown in Figure 10b are expected to be responsible for the hydrogen adsorption in the above potential range.

Potential-Dependent Dynamics of K^+ Complexation. The relative ease with which the highly resolved image of the K^+ adlayer was obtained stimulated us to use this system to study

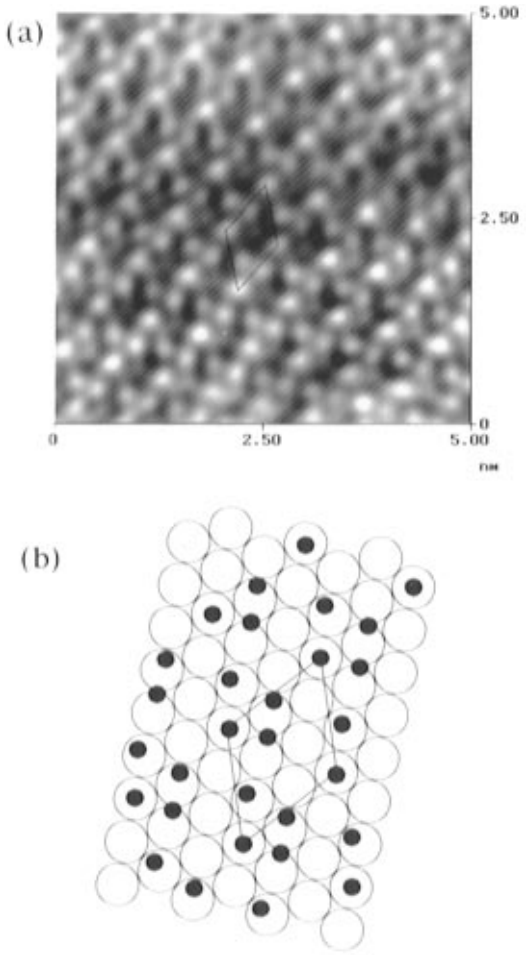

Figure 10. A high-resolution STM image obtained at 0.3 V, and a ball model of the $(\sqrt{7}\times\sqrt{7})$R19° CN structure.

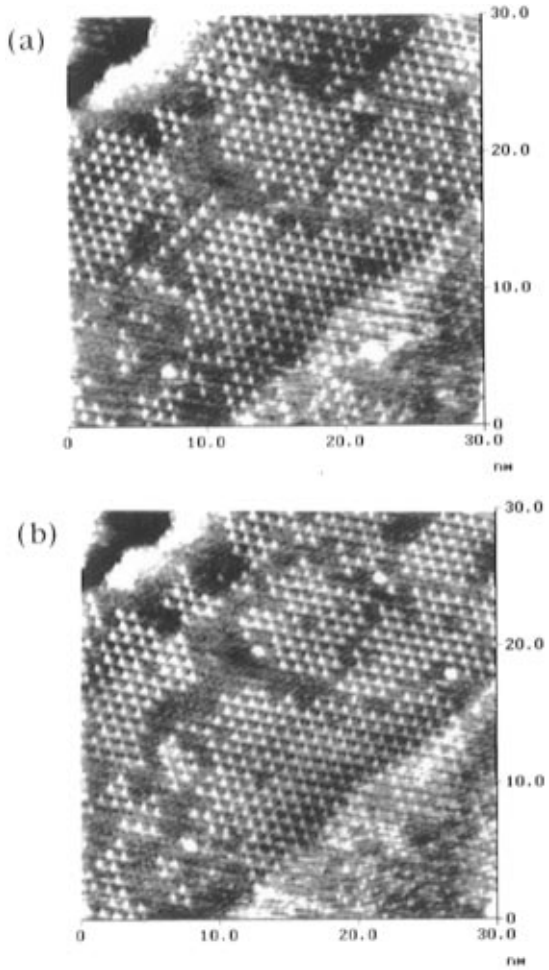

Figure 11. Time-dependent STM images of the Pt(111) electrode in 0.1 mM KCN + 0.1 M $KClO_4$ (pH 9.5). The Pt electrode was held at 0.6 V, and the two images were acquired consecutively with a 20 s difference in time.

the potential effect on the double layer structure. The experimental conditions were identical to those of Figure 6. We focused on the STM imaging in the potential range between 0.75 and 0.5 V, where a small hump appears in the CV (dotted line in Figure 2b). As shown in Figure 6a, almost all hexagonal rings seemed to be occupied by K^+ at 0.6 V. However, it was interestingly found that the number of bright center spots seemed to decrease when the electrode potential was scanned in the negative direction to 0.5 V. The high-resolution STM images shown in Figures 11a and 11b represent a time-dependent structural change at 0.6 V, which corresponds to the peak of the small hump shown in Figure 1b. It can be calculated from Figure 11a that K^+ ions are coordinated on ca. 90% of the hexagonal rings at the potential of 0.6 V.

The time difference between Figures 11a and 11b is 20 s. Despite the fact that most of the K^+ cations remain at the same position in Figures 11a and 11b, a small portion of the K^+ cations have disappeared in Figure 11a, while the remainder appear at the lower left-hand corner of Figure 11b, forming new $2\sqrt{3}$ domains. These rearrangements of K^+ cations could be due to either a migration of the adsorbed K^+ in the CN adlayer or a slow adsorption−desorption dynamics on the CN-covered Pt surface involving K^+ and hydromium cations in solution. Figure 12a was acquired immediately after the electrode potential was stepped from 0.6 to 0.5 V. The image shown in Figure 12b was acquired after 16 min. Clearly resolved monatomic steps were employed as markers to guide against thermal drift in the acquisition of sets of STM images. It can be seen that the population of K^+ rapidly decreased to ca. 50% of the original number within 1 min after the potential step. The vanishing rate of K^+, however, sharply decreased, and it took quite a long time to eliminate all K^+. The coverage of K^+ decreased to less than 10% after 16 min as shown in Figure 12b.

It is expected that the disappearance of the bright center spot is due to the desorption of the coordinated K^+, replaced by a hydronium cation, because high-resolution STM images acquired after the complete desorption of K^+ were very similar to those shown in Figure 9. The exchange rate seemed to be controlled by the diffusion of hydronium cations. The slow vanishing of K^+ is expected to be due to a consequence of the low concentration of protons in the pH 9.5 solution. On the other hand, it was found that the ordered $2\sqrt{3}$ pattern of the adsorbed K^+ cations readily recovered within 2 min when the electrode potential was stepped back from 0.5 to 0.6 V, because of the relatively high concentration of K^+ in solution.

Finally, it is noteworthy that the well-ordered $2\sqrt{3}$ structure underwent reconstruction when the potential was made more negative than 0.2 V. A (2×2) structure appeared as islands. Interestingly, we have also observed relatively large pits in the Pt(111)−(1×1) lattice image, indicating that a partial desorption of CN occurred at 0.2 V as expected from the CV shown in Figure 1b. Although STM images acquired at this potential could be interpreted as a (2×2) structure, it was difficult to achieve high resolution probably because of a fast surface diffusion of the adsorbed CN. The appearance of a (2×2) structure was briefly mentioned in the previous STM study.[7] It is more important to note that the present experiments

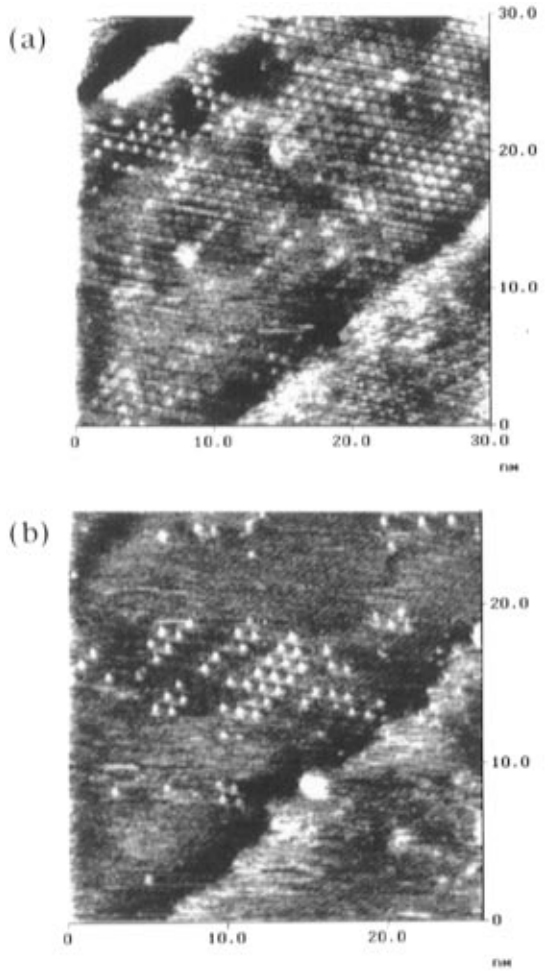

Figure 12. Two consecutive STM images (following Figure 11) obtained after the potential was stepped negatively from 0.6 to 0.5 V. Part **b** was acquired 16 min after part **a**.

were conducted to try to find the $(\sqrt{13}\times\sqrt{13})$R14° structure observed by Hubbard and co-workers.[16] They reported that the $(\sqrt{13}\times\sqrt{13})$R14° structure was observed at potentials more negative than −0.45 V vs Ag/AgCl, and the $(2\sqrt{3}\times2\sqrt{3})$R30° structure appeared at potentials between −0.45 and 0.4 V vs Ag/AgCl in solution with a pH of 9.2. However, the $(2\sqrt{3}\times2\sqrt{3})$R30° structure was consistently observed in this study in the potential range between 1.1 and 0.3 V vs RHE (0.2 and −0.6 V vs SCE) in the alkaline solution. The appearance of the (2 × 2) structure occurred at potentials near 0.2 V vs RHE. We believe that the desorption of K^+, newly found in this study as described above, caused a complication in the previous LEED analysis.

The present success in obtaining high-quality STM atomic resolutions of the coadsorbed cations resulted from the rather unique hexagonal structure of the CN adlayer. The cations are physically pinned down in the center of hexagonal rings. In situ observation of cations on Pt modified with other anions such as Br^-[28] and SCN^-[29] may be difficult to make because of the lack of site-selective interaction between cations in solution and anions adsorbed on Pt. The cations are most likely to be mobile on the electrode surface in these cases. For example, Br^- is known to be strongly adsorbed on a Pt(111) electrode, forming a (3 × 3) structure itself,[28] but no ordered array of the countercations was identified in our previous work.[6] The complexation of other cations on the CN adlayer on Pt(111) is of special interest to us.

Conclusion

In situ STM imaging has revealed detailed structures of not only the specifically adsorbed CN layer but also the counter layer of alkali metal cations on a Pt(111) electrode in CN containing media. The specifically adsorbed CN formed well-ordered $(2\sqrt{3}\times2\sqrt{3})$R30°−CN adlattices on Pt(111). The influence of the STM imaging conditions on the CN appearance in the atomic resolution was demonstrated. A new model structure was proposed for the CN adlayer where no CN group is located in the center of the six-membered rings. The six-member CN group formed a unique hollow hexagonal array, which enabled the strong retention of the alkali metal cations of Na^+ and K^+ at the center of the CN hexagons. This interaction was particularly strong for K^+ so that high-quality STM atomic resolution of the adsorbed K^+ cations was easily obtained. In situ STM also revealed the crucial role of the electrode potential in determining the double layer structure. It was found that the desorption of K^+ occurs at potentials more negative than the peak potential (0.62 V) in the charging current−potential curve. K^+ was expected to be replaced by hydronium cation. The adsorption−desorption of K^+ was found to be reversible. The $(\sqrt{7}\times\sqrt{7})$R19° and (2 × 2) structures were found at negative potentials in the acidic and alkaline solutions, respectively. Other structures reported in the literature, such as $(\sqrt{13}\times\sqrt{13})$R14°, were not observed in the present study.

Acknowledgment. We thank the ERATO project for financial support and Dr. Y. Okinaka and Prof. G. Swain (Utah State University) for their help in the writing of this manuscript. Y.-G. Kim would like to acknowledge the support provided by the Korea Science and Engineering Foundation.

JA9521841

(28) Salaita, G. N.; Stern, D. A.; Lu, F.; Baltruschat, H.; Schardt, B. C.; Stickney, J. L.; Soriaga, M. P.; Frank, D. G.; Hubbard, A. T. *Langmuir* **1986**, *2*, 828.

(29) Cao, E. Y.; Gao, P. G.; Gui, J. Y.; Lu, F.; Stern, D. A.; Hubbard, A. T. *J. Electroanal. Chem.* **1992**, *339*, 311.